Models	Ssp1-2.6	Ssp5-8.5	Models	Ssp1-2.6	Ssp5-8.5	Models	Ssp1-2.6	Ssp5-8.5
ACCESS-1-5	0	40	E3SM-1-ECA	0	1	IITM-ESM	0	1
ACCESS-CM2	0	5	EC-Eart-CC	0	1	INM-CM4-8	0	1
AWI-CM--MR	0	1	EC-Eart-LR	3	3	INM-CM5-0	0	1
BCC-CSM-MR	0	1	EC-Earth3	57	57	IPSL-CM-LR	5	7
CAMS-CS1-0	0	2	EC-EartVeg	7	8	KACE-1-0-G	0	3
CanESM5	50	50	FGOALS-3-L	1	1	KIOST-ESM	0	1
CanESM5nOE	0	3	FGOALS-g3	4	4	MIROC-ES2L	0	10
CIESM	0	1	FIO-ESM2-0	0	3	MIROC6	0	50
CMCC-CMSR5	0	1	GFDL-CM4	0	1	MPI-ESM-HR	0	1
CMCC-ESM2	0	1	GFDL-ESM4	0	1	MPI-ESM-LR	0	30
CNRM-CM-HR	1	1	GISS-E21-G	0	11	MRI-ESM2-0	5	6
CNRM-CM6-1	6	6	GISS-E21-H	0	10	NESM3	2	2
CNRM-ES2-1	0	5	HadGEM3-LL	1	4	NorESM2-LM	1	1
E3SM-1-1	0	1	HadGEM3-MM	1	4	NorESM2-MM	1	1

Supplementary Table 1. CMIP6 models used in this study and the number of members used per each model for the SSP1-2.6 and SSP5-8.5 ensembles.

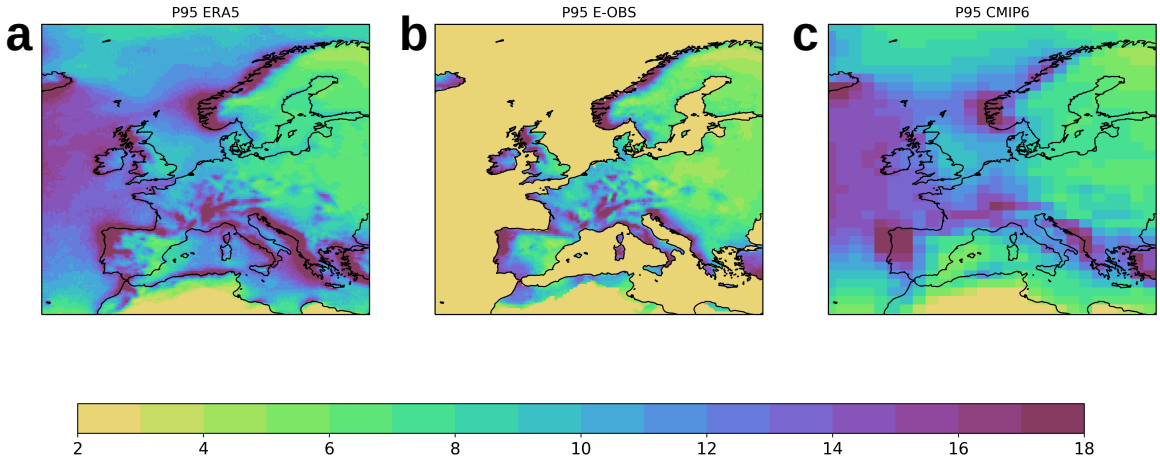

Supplementary Figure 1. 95th percentile of daily precipitation (P95) for the winter (DJF) season from (a) ERA5, (b) E-OBS and (c) CMIP6 ensemble mean. Units are mm per day.

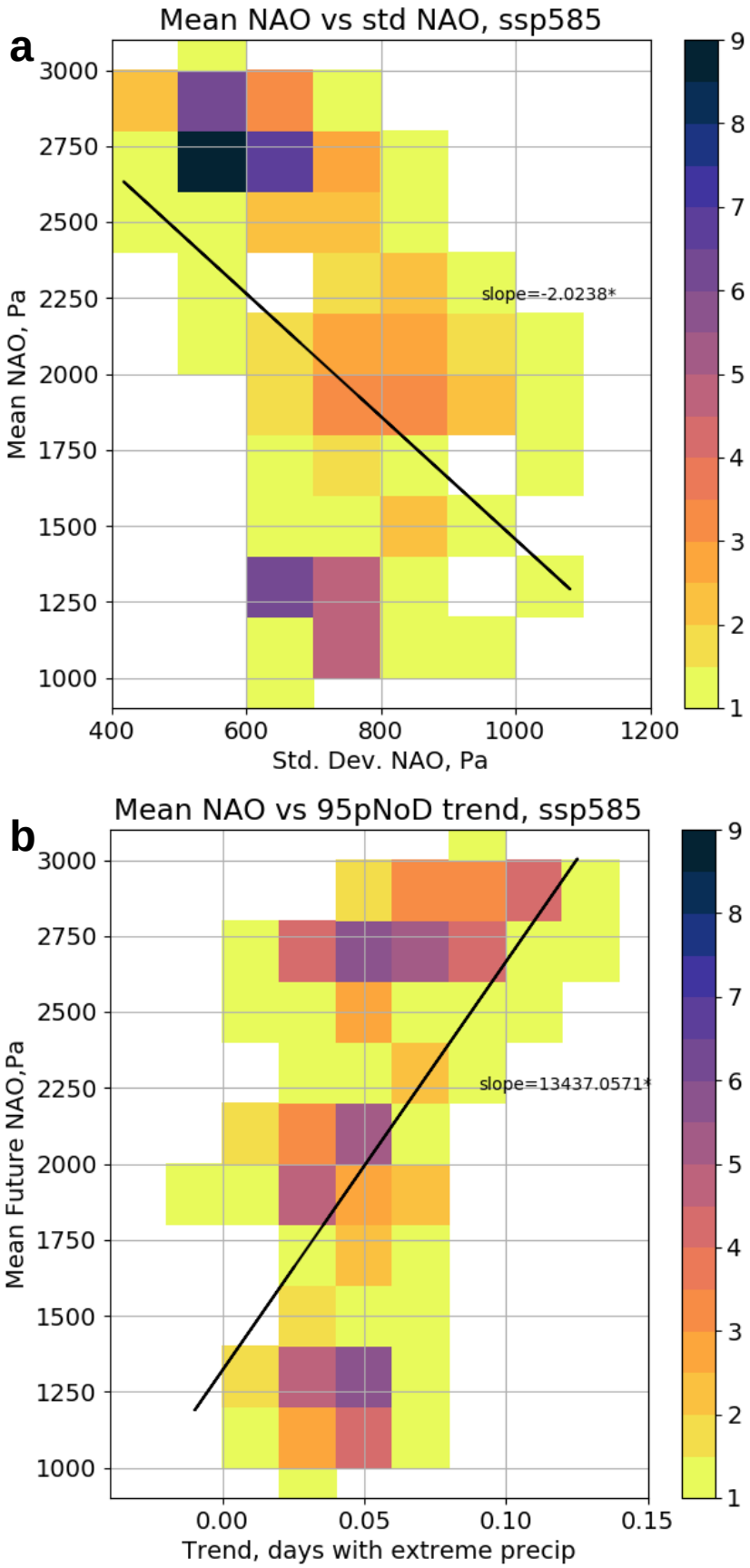

Supplementary Figure 2. Two-dimensional histogram of the a) NAO's standard deviation versus the NAO's mean for the 2050-2099 period for the ssp5-8.5 ensemble. b) Similar to a) for the trend of days with extreme precipitation versus the NAO's mean. Colorbar shows the percentage of models within a bin. The linear regression of both variables is shown for both subplots. The slope of the linear regression is shown in every subplot, and it is marked with an asterisk when the linear regression is significantly different from zero ($p<0.05$).

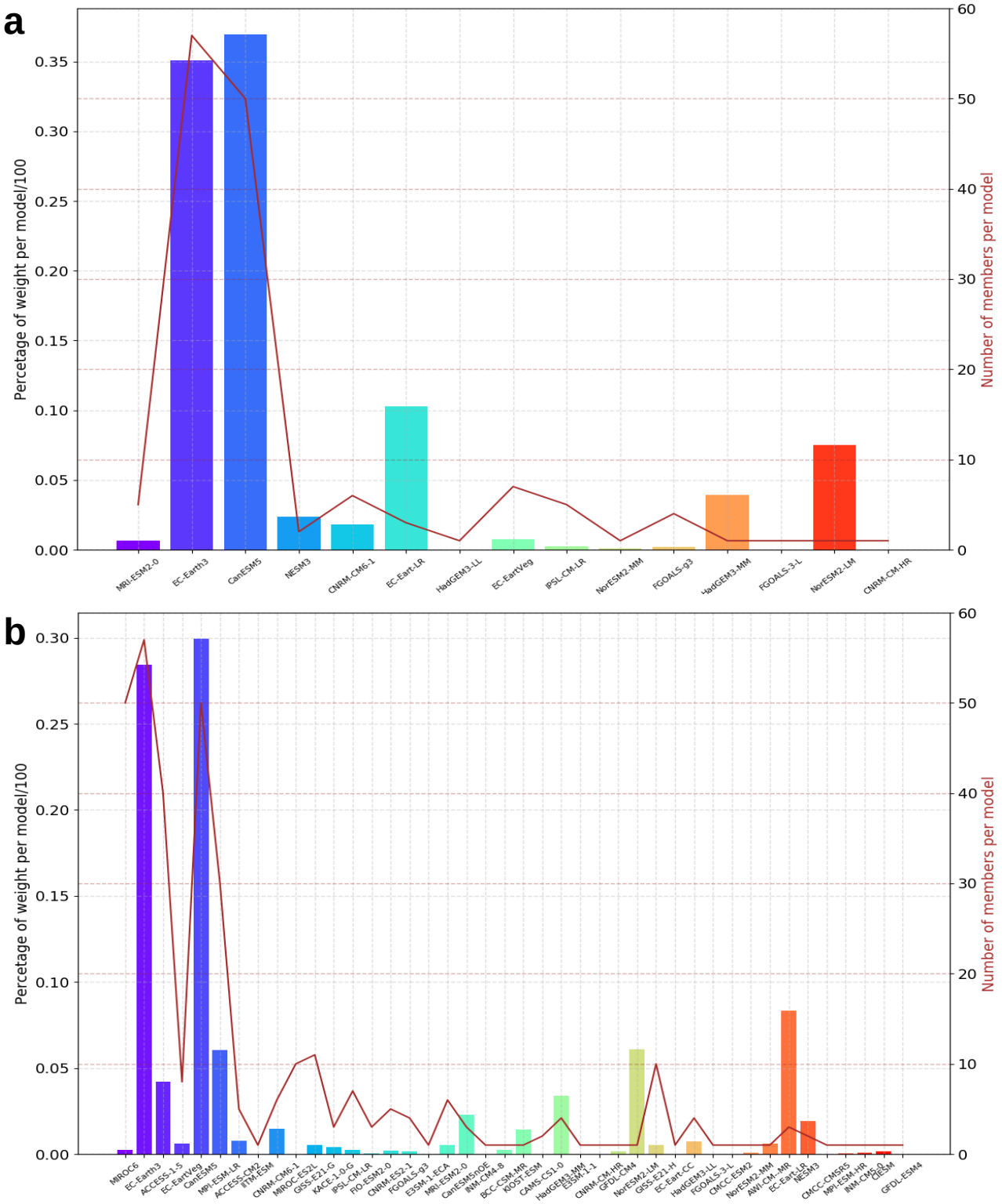

Supplementary Figure 3. Cumulative weight for every model for a) SSP1-2.6 and b) SSP5-8.5 depending on the how similar NAO pattern was compared to ERA5, through the calculation of the MSE of the regression of the index onto the sea level pressure. The method for assigned the weight is described in the methods section. The left y-axis shows the relative percentage of weight given to a certain model, due to adding all its members. The right y-axis shows the number of members per model. The sum of all bars for every subplot equals 1.

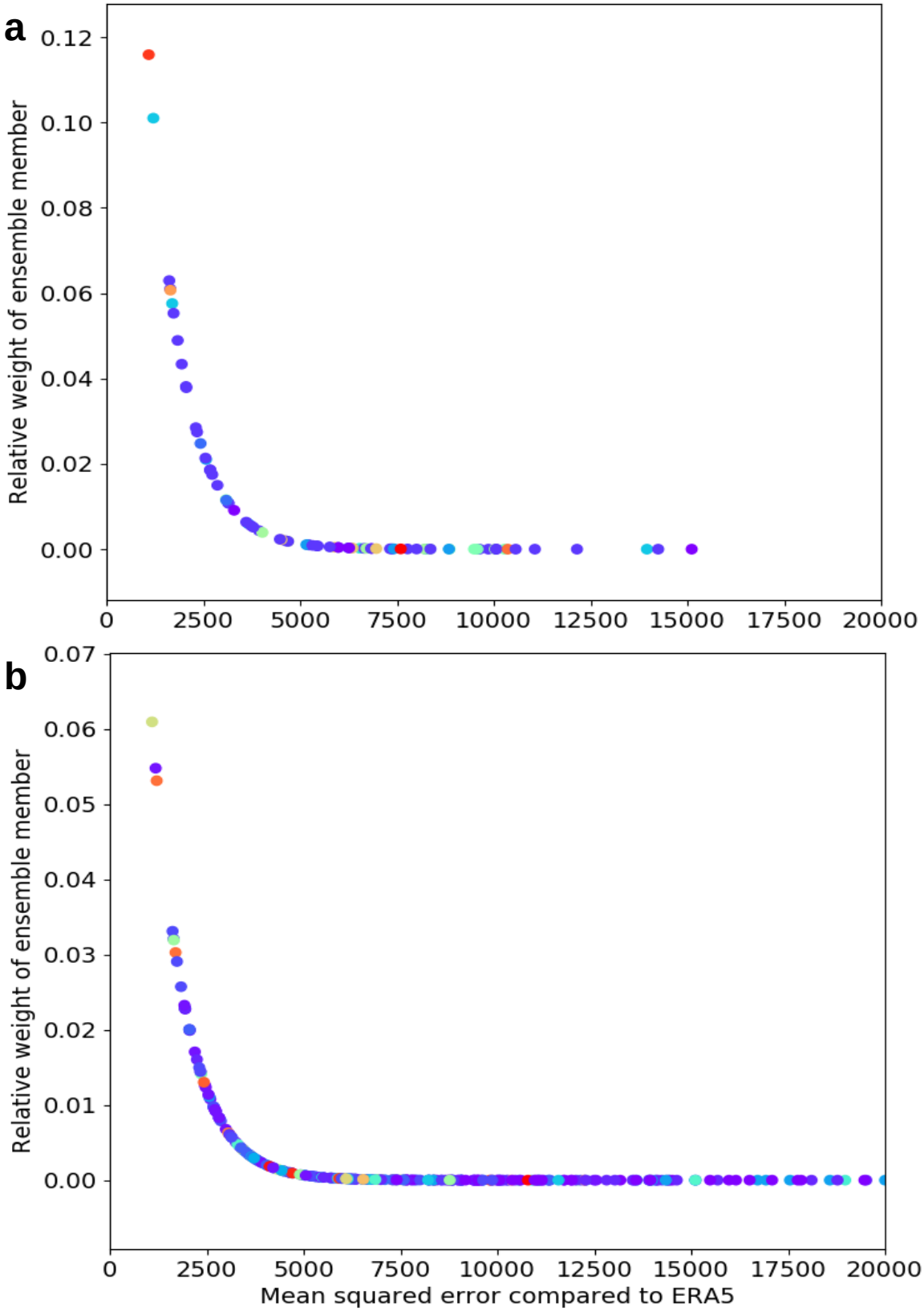

Supplementary Figure 4. Weight given to different model members using eq. 1 described in the method's section for the a) SSP1-2.6 and b) SSP5-8.5. The colors correspond to the respective model bar in SM's Figure 1.

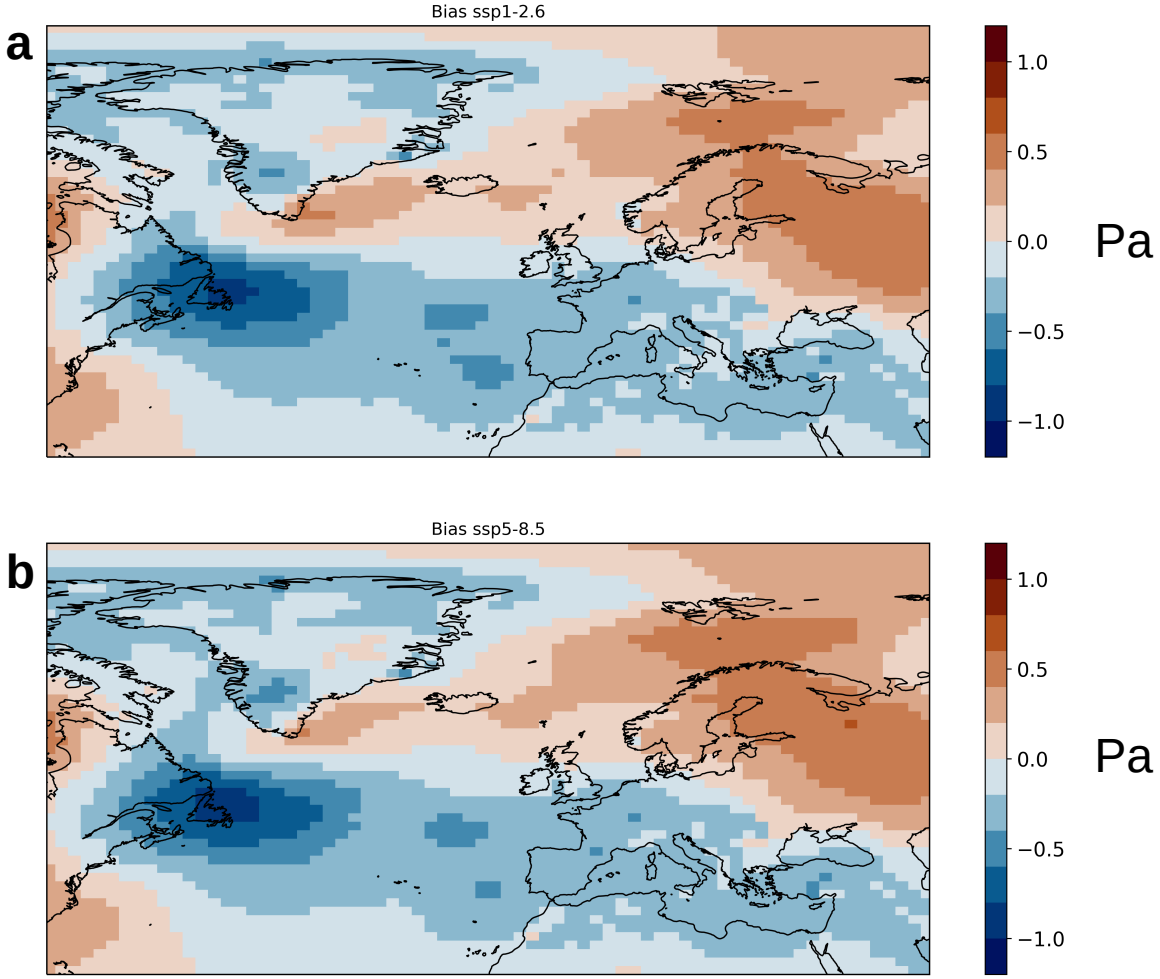

Supplementary Figure 5. Difference (bias) in the regression of psl onto the standardized NAO index between the weighted CMIP6 model ensemble mean and ERA5, for the a) SSP1-2.6 and b) SSP5-8.5 ensembles. The difference was calculated 1970-2014 period.

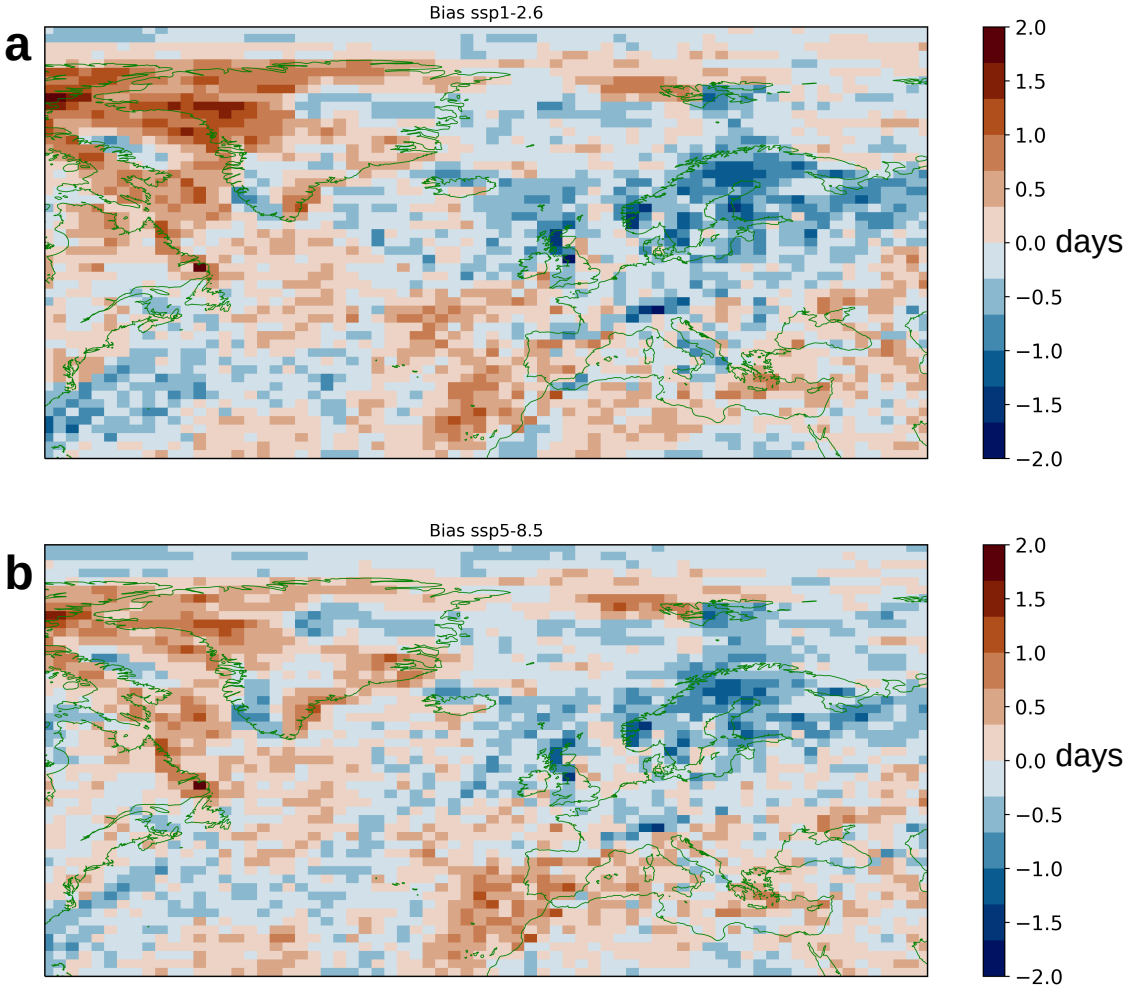

Supplementary Figure 6. Difference (bias) in the regression of 95pNoD onto the standardized NAO index between the weighted CMIP6 model ensemble mean and ERA5, for the a) SSP1-2.6 and b) SSP5-8.5 ensembles. The difference was calculated 1970-2014 period.

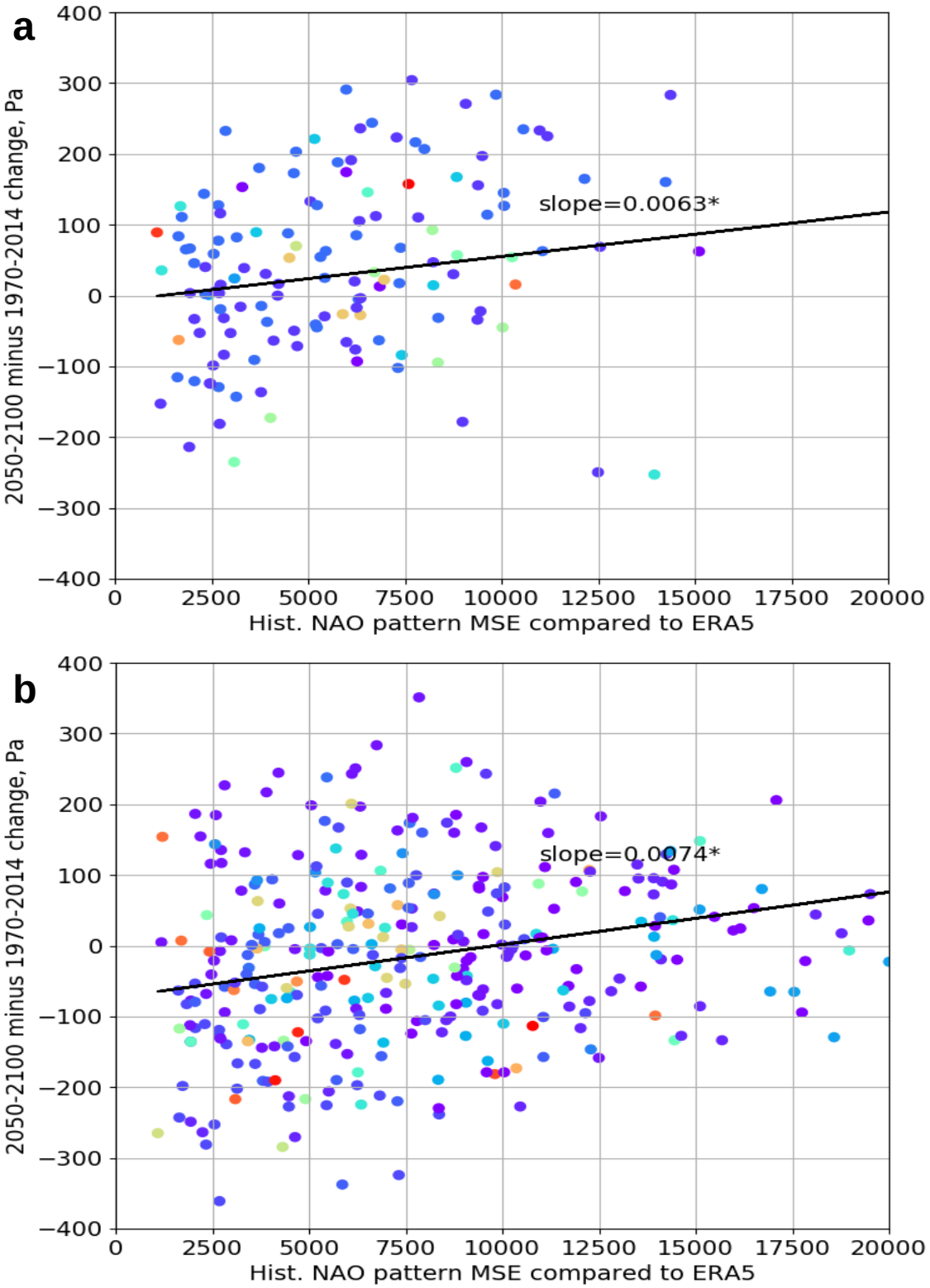

Supplementary Figure 7. Scatter plot of the NAO MSE and the psl gradient between the subtropical (31.5W–24.5°W,36.5°N–40°N) minus the subpolar (25°W–13°W, 63°N–67°N) Atlantic for the a) SSP1-2.6 and b) SSP5-8.5 ensembles. The MSE was calculated as described in the methods section. The psl gradient was calculated from subtracting the spatial average on the subtropical region minus the subpolar regions of the psl regressed onto NAO index. The slope of the linear regression is shown in every subplot, and it is marked with an asterisk when the linear regression is significantly different from zero ($p<0.05$). The colors correspond to the respective model bar in SM's Figure 1.

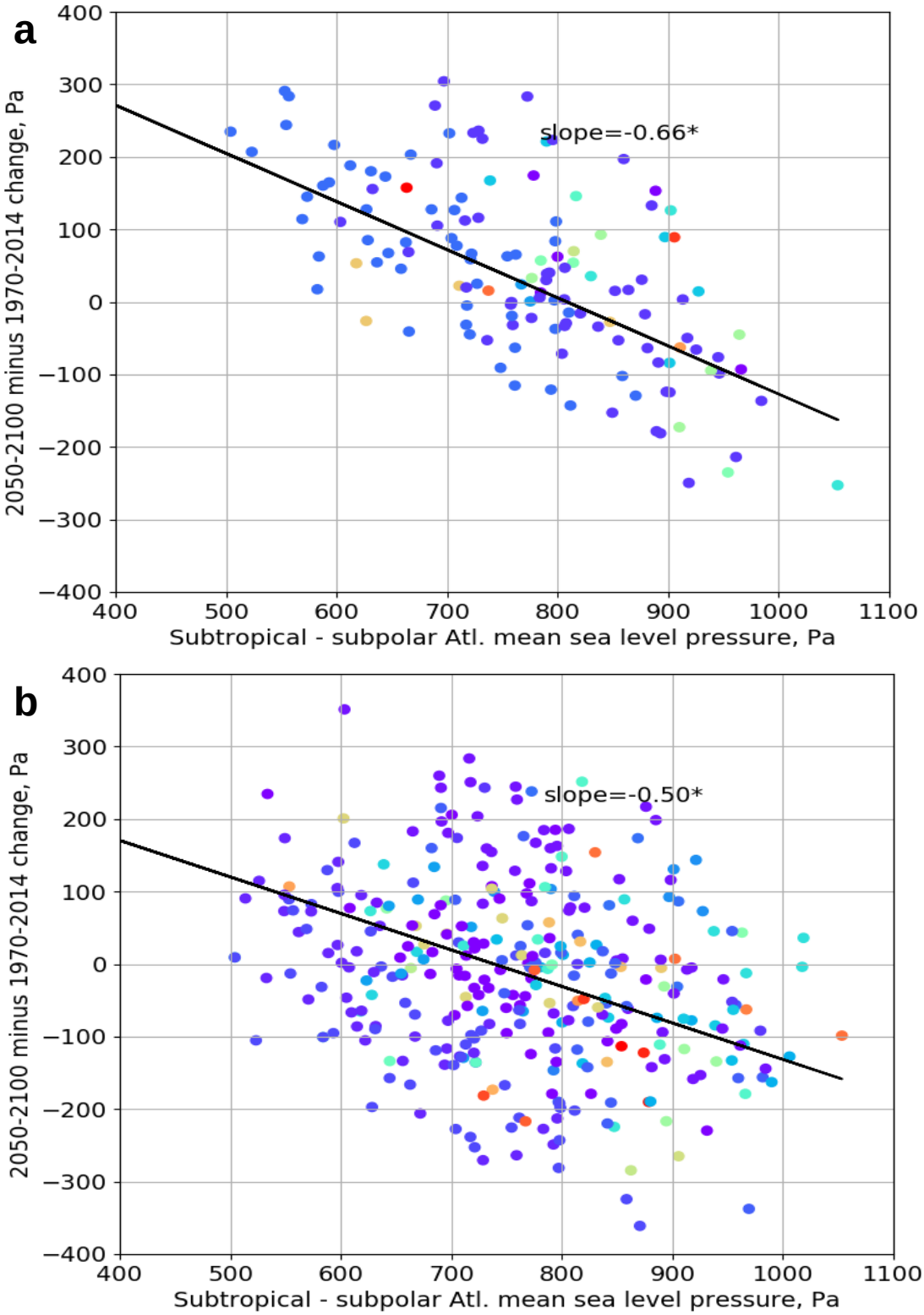

Supplementary Figure 8. Scatter plot of the psl gradient between the subtropical (31.5W–24.5°W,36.5°N–40°N) minus the subpolar (25°W–13°W, 63°N–67°N) Atlantic in the 1970-2014 period and its change in the 2050-2100 period, for the a) SSP1-2.6 and b) SSP5-8.5 ensembles. The slope of the linear regression is shown in every subplot, and it is marked with an asterisk when the linear regression is significantly different from zero ($p<0.05$). The colors correspond to the respective model bar in SM's Figure 1.

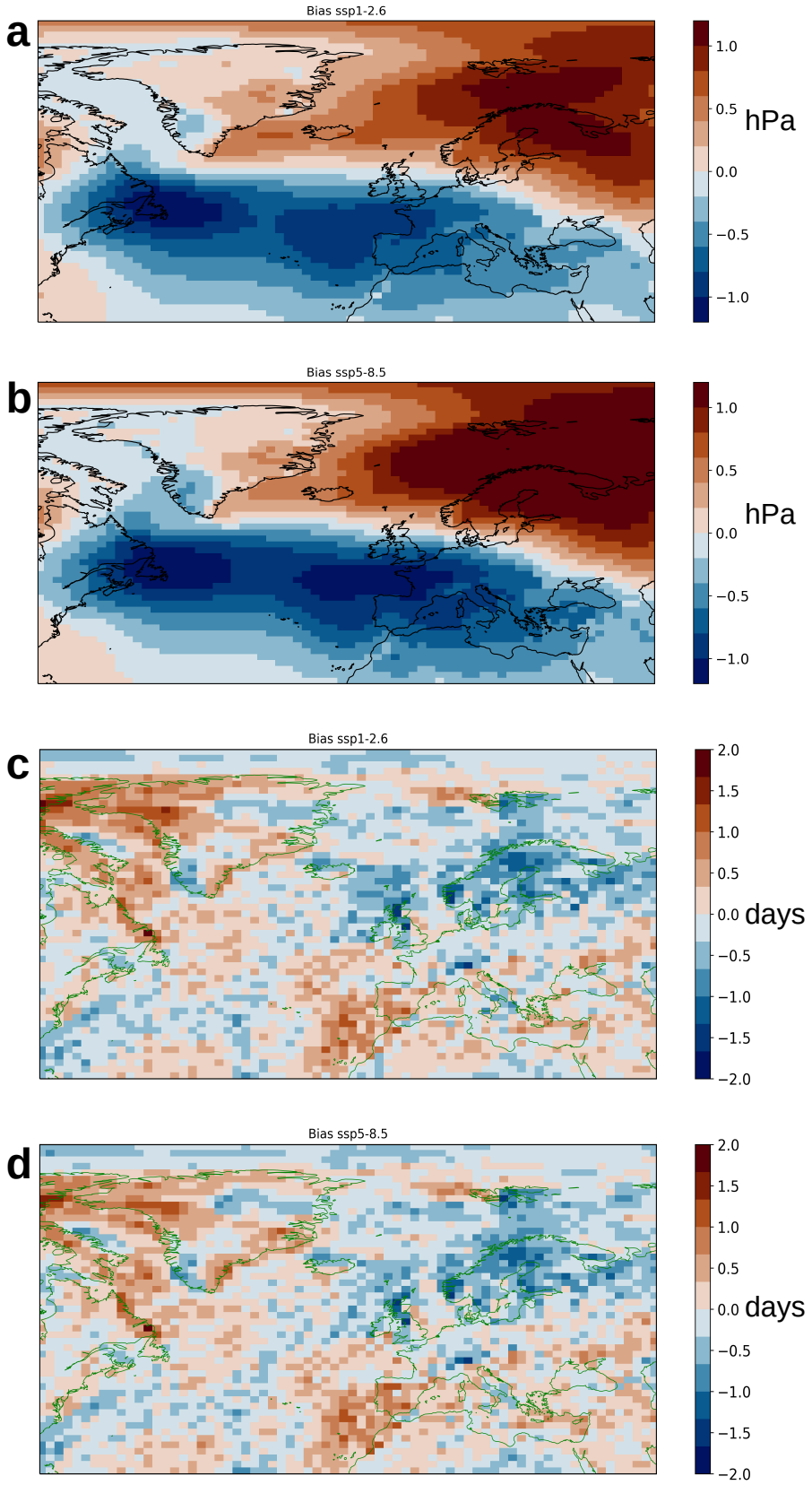

Supplementary Figure 9. Difference (bias) in the regression of psl onto the standardized NAO index between the CMIP6 model ensemble mean and ERA5, for the a) SSP1-2.6 and b) SSP5-8.5 ensembles. Similarly to c) and d) similarly to a) and b) for 95pNoD.The difference was calculated 1970-2014 period. The ensemble mean was calculated with same weights for all the members of the ensemble.

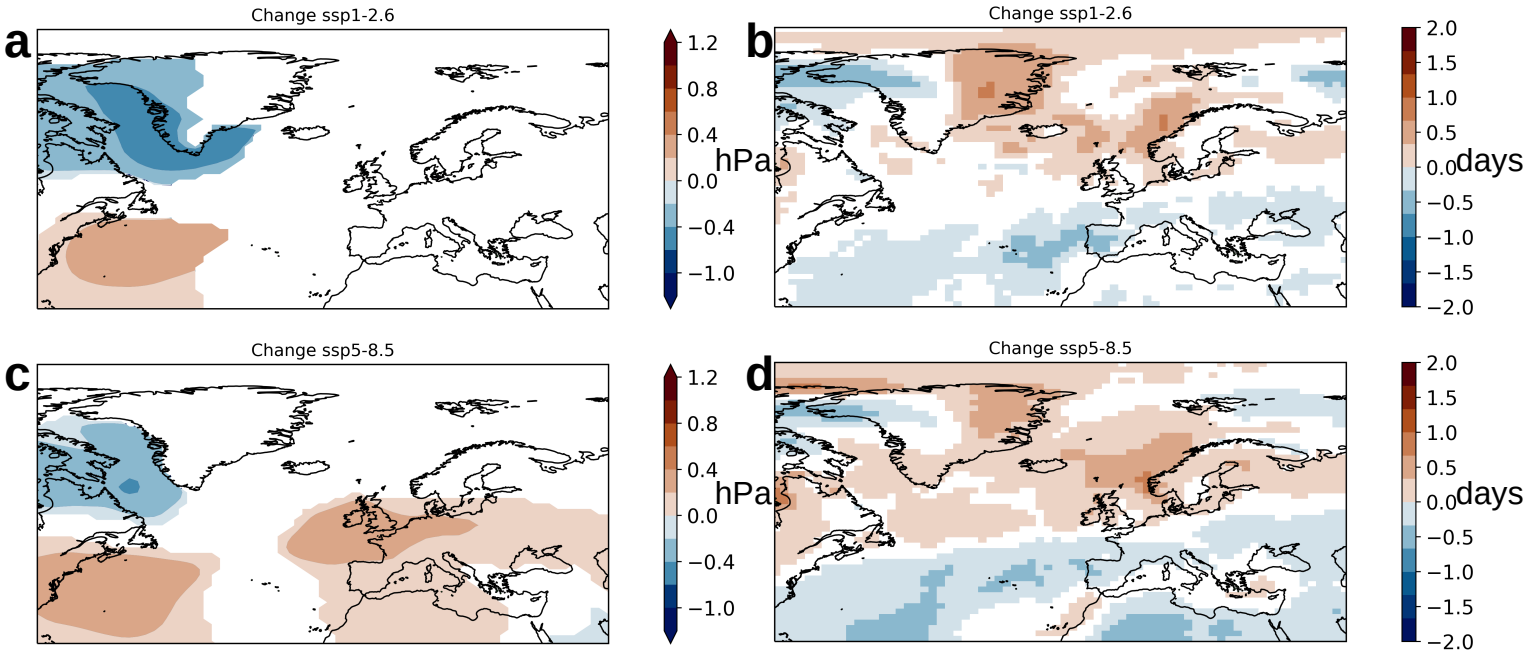

Supplementary Figure 10. Difference of the regression of psl onto the standardized NAO index in the 2050-2099 period minus the 1970-2014 period for the a) SSP1-2.6 and c) SSP5-8.5 ensembles. b) and d) similar to a) and c) for 95pNoD. Units for psl are the hPa and for 95pNoD are the number of days. For 95pNoD, the regression was performed after detrending the NAO and 95pNoD data. In contrast to Fig. 5, for this figure the ensemble mean was calculated with same weights for all the members of the ensemble. Contours show significant ($p<0.01$) changes in the regression values compared to the historical period. The significance for the change in the regression values was calculated with a t-test, with the null hypothesis that two independent correlation values from the historical and future periods in every ensemble have identical average values.

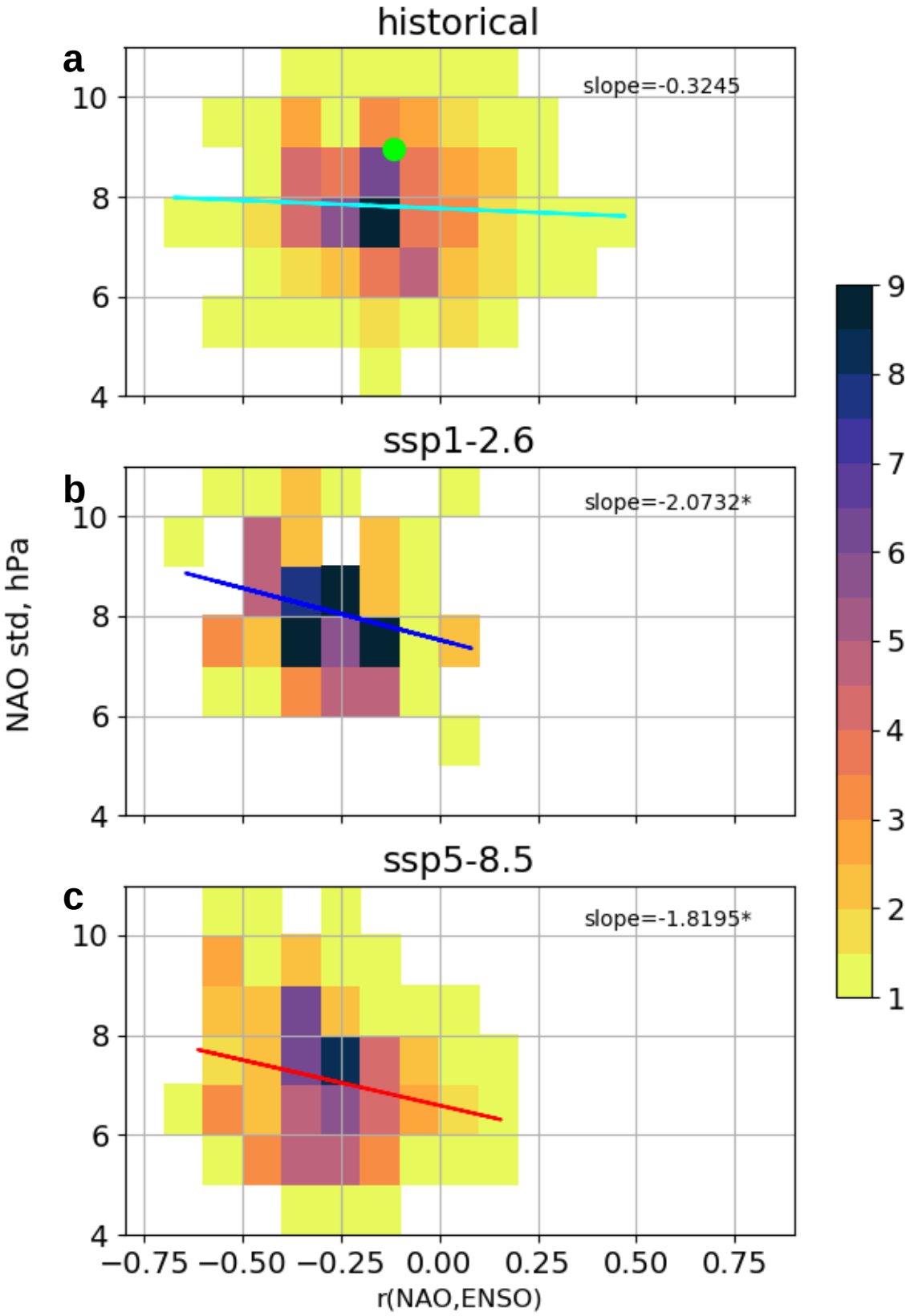

Supplementary Figure 11. Two-dimensional histogram of the NAO's standard deviation versus the ENSO-NAO correlation for a) the 1970-2014 period, the 2050-2099 period for b) the ssp1-2.6 ensemble and c) the ssp5-8.5 ensemble. Colorbar shows the percentage of models within a bin. The linear regression of both variables is shown for the three subplots. The slope of the linear regression is shown in every subplot, and it is marked with an asterisk when the linear regression is significantly different from zero ($p<0.05$). ERA5 is shown with a green scatter point in the historical (upper) subplot.

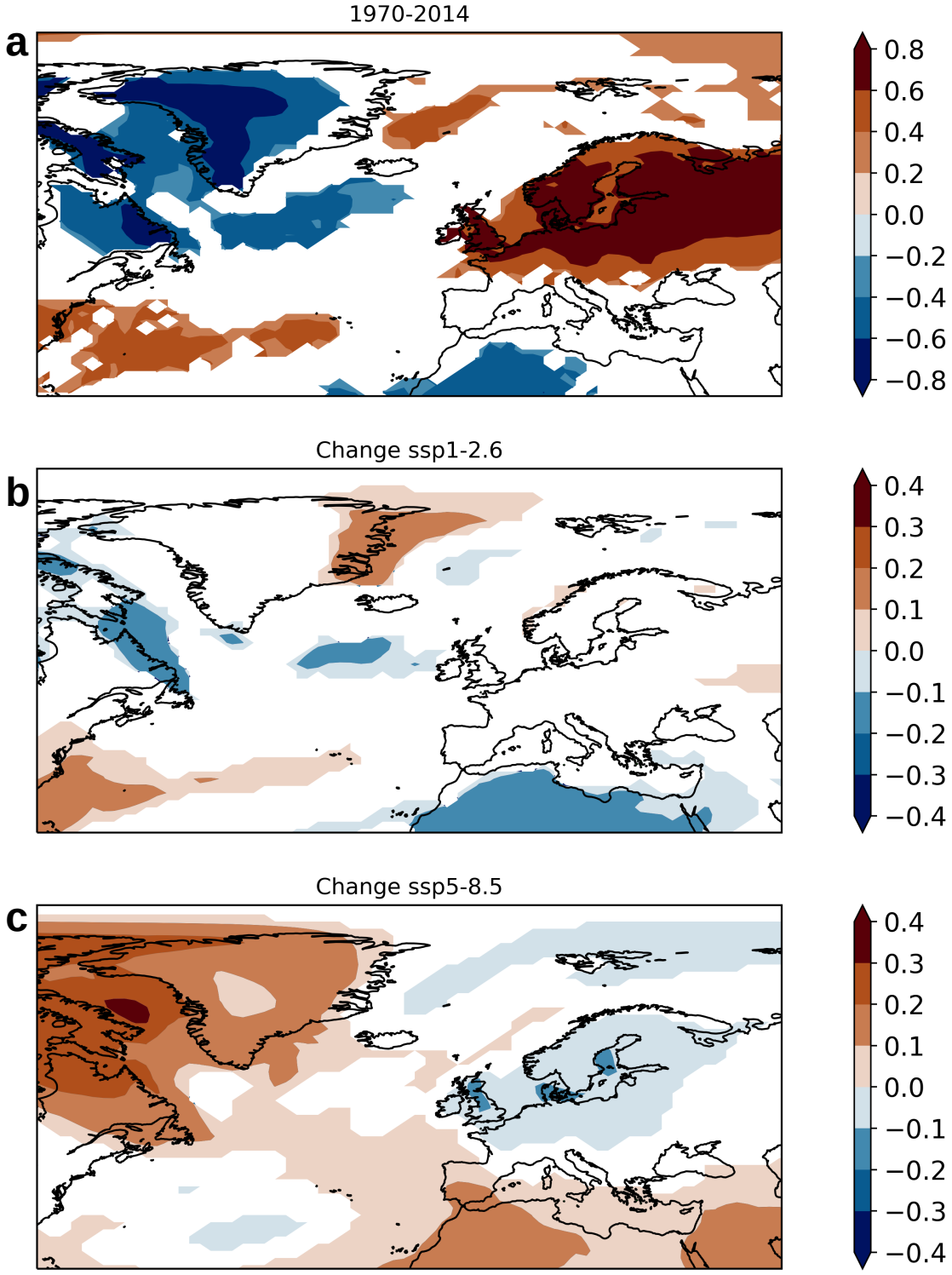

Supplementary Figure 12. Pearson correlation between the NAO index and the skin temperature for ERA5 reanalysis in a) the 1970-2014 period, changes on the correlation pattern between the 2050-2099 and 1970-2014 period are shown for b) the ssp1-2.6 ensemble and c) the ssp5-8.5 ensemble. Contours only show significant correlation values ($p<0.01$) and significant ($p<0.01$) changes in the correlation patterns. The significance for the change in the correlation patterns was calculated with a t-test, with the null hypothesis that two independent correlation values from the historical and future periods in every ensemble have identical average (expected) values.

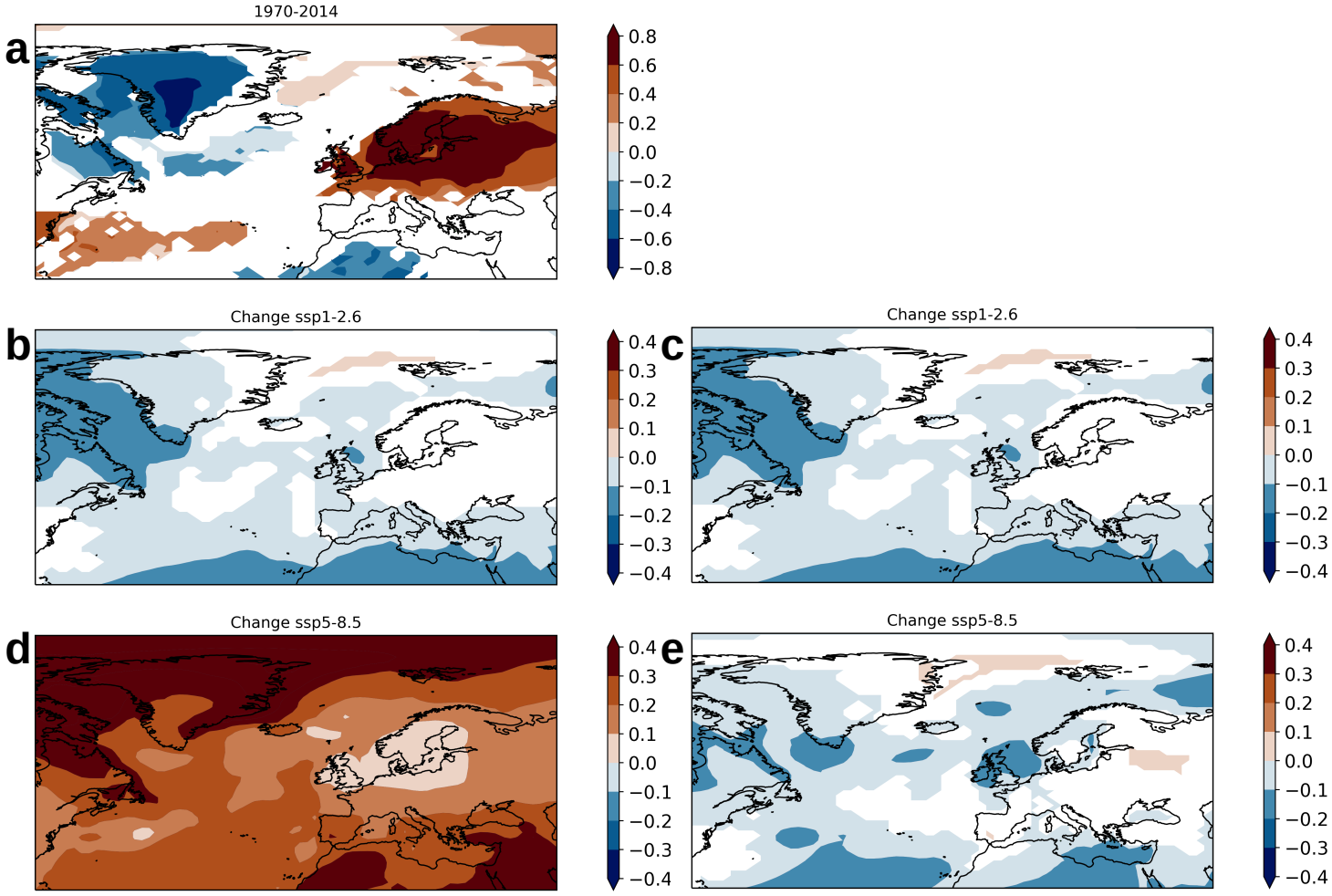

Supplementary Figure 13. Pearson correlation between 95pNoD and the skin temperature for ERA5 reanalysis in the 1970-2014 period (a), changes on the correlation pattern between the 2050-2099 and 1970-2014 period are shown for the ssp1-2.6 ensemble (b) and the ssp5-8.5 ensemble (d). (c) and (e) similar to (b) and (d) performing the Pearson correlation after removing the trends in both 95pNoD and the skin temperature. Contours only show significant correlation values ($p<0.01$) and significant ($p<0.01$) changes in the correlation patterns. The significance for the change in the correlation patterns was calculated with a t-test, with the null hypothesis that two independent correlation values from the historical and future periods in every ensemble have identical average (expected) values.